Article

Ultrasensitive Assay for Telomerase Activity via Self-enhanced Electrochemiluminescence Ruthenium Complex doped Metal-Organic Frameworks with High Emission Efficiency

Chengyi Xiong, Wenbin Liang, Yingning Zheng, Ying Zhuo, Yaqin Chai, and Ruo Yuan

Anal. Chem., **Just Accepted Manuscript** • DOI: 10.1021/acs.analchem.7b00259 • Publication Date (Web): 14 Feb 2017

Ultrasensitive Assay for Telomerase Activity *via* Self-enhanced Electrochemiluminescence Ruthenium Complex doped Metal-Organic Frameworks with High Emission Efficiency

Chengyi Xiong,[1] Wenbin Liang,[1,2] Yingning Zheng,[1] Ying Zhuo,[1] Yaqin Chai[1], Ruo Yuan*[1].*

[1]Key Laboratory of Luminescent and Real-Time Analytical Chemistry (Southwest University), Ministry of Education, College of Chemistry and Chemical Engineering, Southwest University, Chongqing 400715, PR China

[2]Department of Clinical Biochemistry, Laboratory Sciences, Third Military Medical University, 30 Gaotanyan Street, Shapingba District, Chongqing 400038, China.

Abstract

Here, an ultrasensitive "off-on" electrochemiluminescence (ECL) biosensor was proposed for the determination of telomerase activity by using self-enhanced Ruthenium-polyethylenimine (Ru-PEI) complex doped zeolitic imidazolate framework-8 (Ru-PEI@ZIF-8) with high ECL efficiency as ECL indicators and an enzyme-assisted DNA cycle amplification strategy. The Ru-PEI@ZIF-8 nanocomposites were synthesized by self-enhanced Ru-PEI complex doping during the growth of zeolitic imidazolate framework-8 (ZIF-8), which presented high ECL efficiency and excellent stability. Furthermore, owing to porosity of Ru-PEI@ZIF-8, the self-enhanced Ru-PEI complex in the outer layer and inner layer of self-enhanced Ru-PEI@ZIF-8 could be excited by electron causing the utilization ratio of self-enhanced ECL materials could be remarkably increased. To further improve the sensitivity of proposed biosensor, the telomerase activity signal was converted into the trigger DNA signal which was further amplified by an enzyme-assisted DNA recycle-amplification strategy. The proposed ECL biosensor presented great performance for telomerase activity detection from 5×10^{1} to10^{6} Hela cells with a detection limit of 11 cells. Moreover, this method was applied in the detection of telomerase activity from cancer cells treated with anticancer drug, which indicated the proposed method held potential application value as an evaluation tool in anticancer drug screening.

KEYWORDS: Telomerase; Electrochemiluminescence; Metal organic frameworks, Self-enhanced.

Introduction

Telomeres are composed of sequence-specific DNA binding proteins to highly repetitive DNA sequences. They cap the ends of eukaryotic chromosomes and ensure these chromosomes ends are not perceived as DNA double-strand breaks.[1-4] Importantly, they play key role in long-term telomere maintenance and protection.[5-8] In normal cells, progressive telomere shortens and collapses after cell divisions, and then, telomerase was inactivated. However, in cancer cells, telomerase could not be inactivated after cell divisions. Therefore, telomerase has been considered as efficient tumor biomarker to monitor cell carcinogenesis and a high sensitive detection assays to monitor telomerase activity has positive significance for the early cancer evolution. However, traditional analytical methods, such as colorimetric method,[9,10] fluorescent assay,[11-14] electrochemistry,[15-17] polymerase chain reaction-based telomeric repeat amplification protocol and its derivative assays,[18,19] may be limited by relatively low sensitivity and long detection time. Thus, it is urgent to developed ultrasensitive measuring assay for the detection of telomerase activity.

Electrochemiluminescence (ECL) as a combination of electrochemistry and chemiluminescence has attracted much attention in analytical chemistry due to its high sensitivity and high controllability.[20-22] To further improve sensitivity of ECL technology, several kinds of luminophores with high luminescence efficiency, such as carbon quantum dots,[23,24] silver nanocluster[25] and self-enhanced ECL material,[26-28] have been introduced into the construction of ECL analytical systems in recent years. In our previous research reports, self-enhanced ECL reagents with luminophore and coreactive group inside a same molecule could generate high ECL responses and improve emission efficiency due to the intramolecular reaction with effectively shorter electronic transmission distance, higher the ECL reaction probabilities

and lower the energy loss compared with the intermolecular reaction.[26,27] Although the reported luminophores presented superior ECL efficiency, only the outer layer of luminophores immobilized on the eletrode could be excited by electron resulting in the low utilization ratio and poor stability of ECL luminophores, which limited their application in ECL. In recent years, some groups introduced metal-organic frameworks (MOFs) into the construction of luminescence analysis method.[29-32] The luminescence-functionalized MOFs could increase the immobilized amount and the stability of luminophores owing to the large specific area and stable structure of MOFs, which improved the sensitivity and stability of ECL luminophores in a certain extent. However, the non-conductive shell of MOFs might prevent electron to excite the luminophores causing the utilization ratio of ECL luminophores was still limited. Therefore, it was a challenge to find a way to increase the stability and utilization ratio of ECL luminophores in MOFs.

Herein, an ultrasensitive "off-on" ECL biosensor was proposed for the determination of telomerase activity by using self-enhanced Ruthenium-polyethylenimine (Ru-PEI) complex doped zeolitic imidazolate framework-8 (Ru-PEI@ZIF-8) as efficient ECL indicators and an enzyme-assisted DNA cycle amplification strategy. Briefly, tris (4,4'-dicarboxylicacid-2,2'-bipyridyl) ruthenium(II) dichloride ($Ru(dcbpy)_3^{2+}$) was linked with polyethylenimine (PEI) through amide bond, forming self-enhanced Ru complex (Ru-PEI). Afterward, Ru-PEI@ZIF-8 was synthesized by self-enhanced Ru-PEI complex doping during the growth of ZIF-8. The self-enhanced Ru-PEI complex with many secondary amine groups in its molecular skeleton could coordinate with the Zinc ion (Zn^{2+}), which was the central ion of ZIF-8. Therefore, the self-enhanced Ru-PEI complex could not only be encapsulated inside of ZIF-8, but also cover the surface of ZIF-8, which remarkably increased the immobilization amount of self-enhanced Ru-

PEI complex. And owing to the porosity of Ru-PEI@ZIF-8, self-enhanced Ru-PEI complex in the outer layer and inner layer of Ru-PEI@ZIF-8 could be excited by electron causing the utilization ratio and stability of self-enhanced Ru-PEI complex could be remarkably increased by the introducing of ZIF-8. As shown in Scheme 1A, the telomerase activity signal was converted to trigger DNA signal firstly. For further improvement of sensitivity, an enzyme assisted DNA recycle-amplification strategy was introduced to amplify trigger DNA signal. In the presence of telomerase and deoxyribonucleoside triphosphates (dNTPs), the telomerase primer that was immobilized on the surface of Fe_3O_4 nanoparticles (Fe_3O_4 NPs) could be extended with repetitive nucleotide sequences (TTAGGG), which could open the hairpin structure of hair probe (HP) and partially hybridize with HP. After that, the hybridized DNA duplexes were digested by exonuclease III (Exo III) and released telomerase primer and trigger DNA. The released extended telomerase primer could trigger another cycle, generating an exponential amplification (cycle I). As shown in Scheme 1B, subsequently, the synthesized Ru-PEI@ZIF-8 and Pt nanoparticles (PtNPs) were dispersed in chitosan (CS) solution (CS/Ru-PEI@ZIF-8/PtNPs). The mixture was dropped in glass carbon electrode (GCE) forming CS/Ru-PEI@ZIF-8/PtNPs film modified GCE with high ECL response. The PtNPs could act as electron channel to promote the electron transfer which might further enhance the ECL of Ru-PEI@ZIF-8. When thiol modified complementary DNA linked with graphene oxide (GO) was immobilized electrode surface through Pt-S bond, the ECL signal of Ru-PEI@ZIF-8 was reduced. Because the GO as black body material could be employed as ECL acceptor to adsorb the light from Ru-PEI@ZIF-8 as ECL donor in ECL resonance energy transfer system (ECL-RET).[33] And the proposed ECL biosensor was turned to an “off” state. After the trigger DNA prepared from cycle I was incubated on the GCE and hybridized with the complementary DNA, the complementary DNA

with GO was nicked by Nb.BbvCI and the trigger DNA was released and triggered another cycle (cycle II). With the leaving of GO, the ECL signal of Ru-PEI@ZIF-8 recovered and the proposed ECL biosensor turned to an "on" state, and the increased ECL signal of the proposed biosensor was associated with the increasing of cell numbers containing different telomerase extract. Owing to the fact that some amplification steps were not operated in the limited space of electrode, the amplification efficiency was improved significantly causing the detection throughput of proposed ECL biosensor was remarkably increased. Through the introducing of Ru-PEI@ZIF-8 and enzyme-assisted DNA cycle amplification strategy, the ECL response of proposed ECL biosensor was greatly enhanced and the sensitivity of the proposed ECL biosensor was significantly improved. As a result, the proposed ECL biosensor presented excellent detection performance to monitor telomerase activity and held great potential in clinical disease diagnose and bioanalysis research.

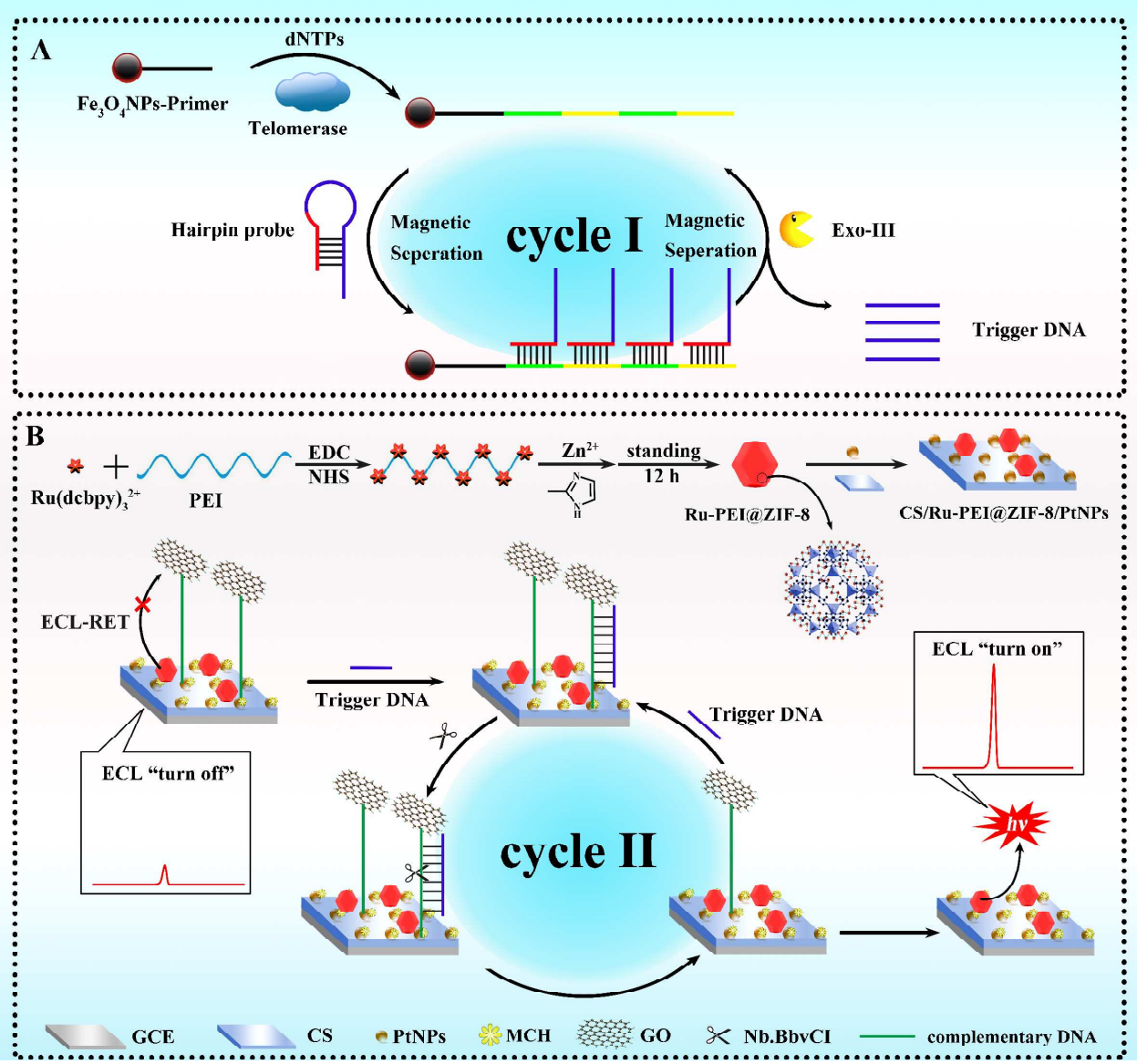

Scheme 1 (A) the preparation of trigger DNA (B) the synthetization of Ru-PEI@ZIF-8 nanocomposite and the construction of proposed ECL biosensor

Experimental

Synthesis of Ru-PEI@ZIF-8

The Ru-PEI@ZIF-8 was synthesized by following steps. Firstly, $Ru(dcbpy)_3^{2+}$ (9 mg) was dissolved in 2 mL ultrapure water. Then, carbodiimide hydrochloride (EDC) (28.8 mg) and N-

hydroxysulfosuccinimide (NHS) (5.8 mg) were added into the $Ru(dcbpy)_3^{2+}$ solution under magnetic stirring with 15 min for activing the carboxyl groups of $Ru(dcbpy)_3^{2+}$. Next, activated $Ru(dcbpy)_3^{2+}$ (2 mL) was reacted with 1 mL PEI solution (1%, *w/w*) for 2 h to synthesize the self-enhanced Ru complex.

At the same time, 5 mL $Zn(NO_3)_2$ solution (25 mM) was mixed with 5 mL 2-methylimidazole (25 mM). After standing for 2 h, 3 mL obtained self-enhanced Ru complex solution was added into the mixture. After standing for 10 h again, Ru-PEI@ZIF-8 was collected by centrifugation and washing several times with ultrapure water. And the final products were dispersed in 10 mL ultrapure water and stored for further used.

Cell Culture and Telomerase Extraction

Hela cells were cultured in DMEM medium supplemented with 10% fetal calf serum and maintained at 37 °C in a humidified atmosphere (95% air and 5% CO_2). Hela cells were collected in the exponential phase and washed twice with ice-cold sterile PBS. After that, 10^6 cells were resuspended in 2 mL of ice cold CHAPS lysis buffer (10 mM Tris-HCl, pH 7.5, 1 mM $MgCl_2$, 1 mM EGTA, 0.5% CHAPS, 10% glycerol, 0.1 mM PMSF) and stored in 4 mL EP tube. And then, the cell lysis was frozen at -80 ˚C for 30 min. Subsequently, the cell lysis was centrifuged for 20 min at 4 ˚C (12000 rpm). The finally clean lysis was stored at -80 ˚C for further used.

Telomerase Extension Reaction and Preparation of Trigger DNA

Firstly, 30 μL of EDC (0.3 mM) solution containing NHS (0.1 mM) were added into 44 μL of telomerase primer (TSP) (100 μM) for activing the carboxyl groups in the terminal of TSP.

And then, the activated TSP were reacted with the amino groups on the surface of Fe_3O_4NPs forming Fe_3O_4NPs-primer.

After above steps, Fe_3O_4NPs-primer (10 μL), telomerase extracts (40 μL), telomerase reaction buffer (10 μL) (20 mM pH 8.3 Tris-HCl buffer, 1 mM EGTA, 0.005% Tween 20, 1.5 mM $MgCl_2$ and 63 mM KCl) and dNTPs solution (10 mM, 10 μL) were mixed in a EP tube. Subsequently, the mixture was incubated at 37 ˚C for 1 h. Sequentially, hairpin probe (2.5 μM, 20 μL) was added into the mixture and opened by the extended parts of TSP after incubating at 37 ˚C for 2 h. Then, Exo III (1 μL, 200 U/μL) with reaction buffer (10 μL) was added to the mixture. The mixture was incubated at 37 ˚C for 6 h. Next, the red part of HP was digested with the aid of Exo III, releasing the blue part of HP as trigger DNA. After magnetic separation, the supernatant containing trigger DNA was stored at 4 ˚C before used.

The fabrication of proposed ECL biosensor

Ru-PEI@ZIF-8 (1 mL), Pt nanoparticles (PtNPs, 1 mL) and Chitosan solution (10 mL, 0.01%, *w/w*) were mixed before the fabrication of proposed biosensor (CS/Ru-PEI@ZIF-8/PtNPs). The fabrication of three electrode system and the pretreatment of working electrode were according to our previous report. After that, 16 μL complementary DNA solution were dropped onto the pretreated GCE and incubated for 12 h at room temperature with dark condition. Through this step, the thiol modified complementary DNA were immobilized on PtNPs via Pt-S bond. Then, the GCE was rinsed with ultrapure water and blocked with MCH (16 μL, 1 mM) for 2 h. Meanwhile, 10 μL EDC solution (3 mg/mL) containing 1 mg/mL NHS was added into GO solution (500 mg/mL) to activate the carboxyl groups of GO under magnetic stirring for 15 min. Then, the GCE was incubated with 16 μL activated GO for 2 h to make GO

link on the terminal amino group of complementary DNA. After incubating for 2 h, the proposed ECL biosensor was successfully fabricated.

ECL Measurement Procedure

To measure the ECL response of the proposed biosensor, the modified GCE was incubated with 16 μL trigger DNA for 2 h. After washing by ultrapure water, the GCE was incubated with 1 μL Nb.BbvCI and 10 μL Nb.BbvCI reaction buffer for another 2 h. After rinsing with ultrapure water to remove extra reagents, the ECL signal of proposed biosensor was measured as our previous report.[26-28]

Results and Discussion

Characteristics of Ru-PEI@ZIF-8

The scanning electron microscope (SEM) was employed to characterize the size and morphology of ZIF-8/PEI-Ru composites. Fig. 1 revealed that the synthesized Ru-PEI@ZIF-8 nanoparticles were defined as rhombic dodecahedron and the diameter was about 500 nm. The EDS mapping revealed that Zn, Ru and Cl were uniform distributed in the synthesized Ru-PEI@ZIF-8 nanoparticles.

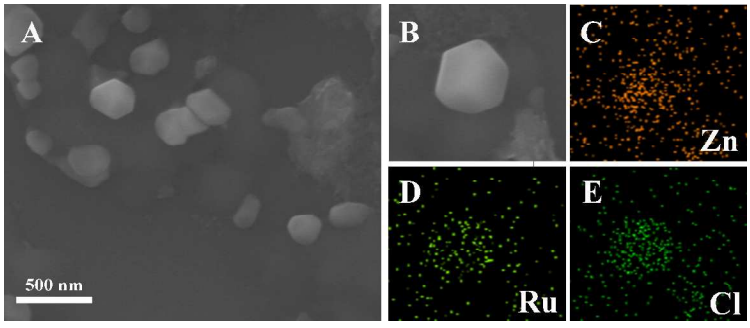

Fig. 1 The SEM images of proposed PEI-Ru @ZIF-8 (A); EDS mapping in SEM for a single Ru-PEI@ZIF-8 nanocomposit (B) with Zn (C), Ru (D) and Cl (E).

To characterize the forming of proposed Ru-PEI@ZIF-8 nanocomposites, X-ray photoelectron spectroscopy (XPS) was employed to characterize the elemental composition of Ru-PEI@ZIF-8. As excepted, the characteristic peaks for Zn2p, O1s, Ru3p, Ru3d, N1s and C1s were obviously presented in Fig. 2. These proof demonstrated that the proposed Ru-PEI@ZIF-8 was successfully synthesized.

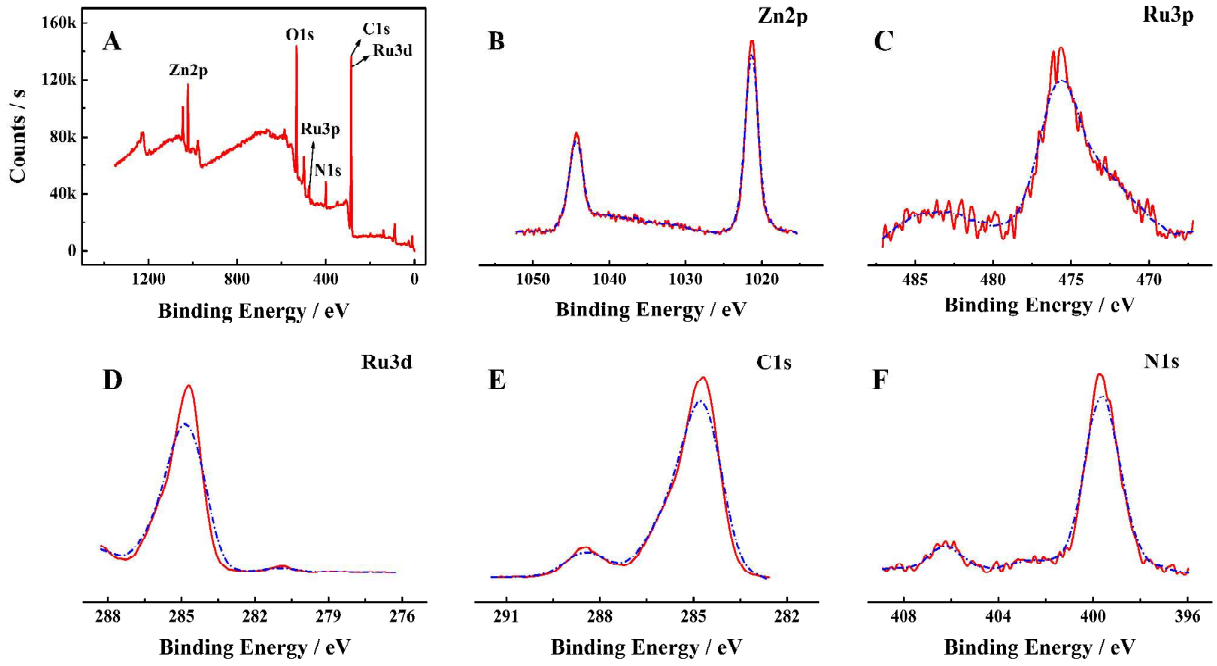

Fig. 2 The XPS analysis for **(A)** proposed Ru-PEI@ZIF-8, **(B)** the Zn 2p region, **(C)** the Ru 3p region, **(D)** the Ru 3d region, **(E)** the C 1s region and **(F)** N 1s region.

The X-ray diffraction (XRD) was applied to further characterize the structure of synthesized Ru-PEI@ZIF-8 nanocomposites. As shown in Fig. S1 (supporting information), the XRD characteristic peaks of ZIF-8 appeared in the XRD patterns of proposed Ru-PEI@ZIF-8 (Table

S2, supporting information), which implied that the doping of $Ru(dcbpy)_3^{2+}$ had nearly little influence on the crystal structure of ZIF-8.

The fluorescent spectrum of proposed Ru-PEI@ZIF-8 was presented in Fig. S2 (supporting information). As anticipated, the fluorescent spectrum of Ru-PEI@ZIF-8 nanocomposites were same as the fluorescent spectrum of $Ru(dcbpy)_3^{2+}$ as previous literature.[26] The maximum excited wavelength of Ru-PEI@ZIF-8 was at λ = 480 nm. And the maximum emission wavelength of Ru-PEI@ZIF-8 was at λ = 609 nm. These results indicated that the Ru-PEI complex were successfully doped in ZIF-8.

ECL characteristics of proposed biosensor

The construction of the proposed ECL biosensor was characterized by ECL measurements after every steps. As shown in Fig. 3, the PtNPs/Ru-PEI@ZIF-8/CS film showed a strong ECL signal, which indicated that the proposed Ru-PEI@ZIF-8 had superior ECL property (curve a). Then, the ECL signal decreased after the addition of complementary DNA and MCH respectively (curve b and curve c). The decreasing of ECL signal was due to the fact that the complementary DNA and MCH could hinder the electron transfer. Afterward, the ECL signal was remarkably decreased when GO was linked with complementary DNA (curve d), because there was energy transfer happened between GO and Ru-PEI@ZIF-8 nanocomposites. The GO as well-known black body material acted as the ECL accepter to absorb the luminescence of Ru-PEI@ZIF-8 nanocomposites as ECL donor in the energy transfer system. Subsequently, the ECL signal further decreased when the electrode was incubated with trigger DNA, because the electron transfer was hindered by trigger DNA (curve e). Finally, the a obviously increasing of ECL signal was observed when the electrode was incubated with Nb.BbvCI. The reason was that

the complementary DNA was nicked by Nb.BbvCI and GO left the electrode surface so that the ECL signal of Ru-PEI@ZIF-8 nanocomposites recovered (curve f). All these results indicated that the proposed ECL biosensor was successfully fabricated.

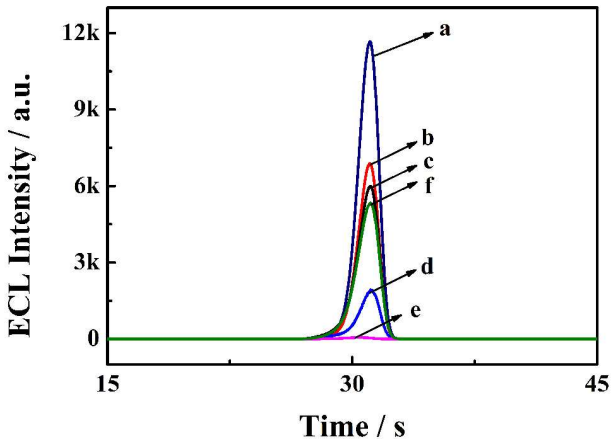

Fig. 3 (A) ECL-times profiles of (a) GCE/CS/Ru-PEI@ZIF-8/PtNPs (b) GCE/CS/Ru-PEI@ZIF-8/PtNPs/complementary DNA; (c) GCE/CS/Ru-PEI@ZIF-8/PtNPs/complementary DNA/MCH; (d) GCE/CS/Ru-PEI@ZIF-8/PtNPs/complementary DNA/MCH/GO; (e) GCE/CS/Ru-PEI@ZIF-8/PtNPs/complementary DNA/MCH/GO/Trigger DNA; (f) The prepared GCE/CS/Ru-PEI@ZIF-8/PtNPs/complementary DNA/MCH/GO/Trigger DNA incubated with Nb.BbvCI in 0.1 M PBS (pH 7.4) with a scanning potential from -1.5 to 1.5 V and at a scan rate of 100 mV s^{-1}.

Detection performance and Stability of proposed biosesnor

The telomerase in Hela cell lysis was detected by proposed ECL biosensor to study the sensitivity. From Fig. 4A, the ECL signal increased linearly with the increasing of logarithm of cell number in the range from 5×10^{1} to 10^{6}. The detection limit was 11 cells at the signal to noise ratio of 3 (S/N = 3). The regression equation was I = 1354.6 (±26.3) lg (cell number) – 1325.6 (±74.8) with a correlation coefficient of R^2 = 0.9970. The results indicated that the

proposed biosensor presented good performance in the detection for telomerase activity and could act as an effective assay for telomerase activity measuring.

The stability of the proposed ECL biosensor was study in this work. As Fig. 4B shown, the ECL response increased with the increasing of Hela cell numbers. A relatively stable ECL response was observed at each cell number. These proofs proved that the proposed ECL biosensor had proper stability for telomerase activity measuring.

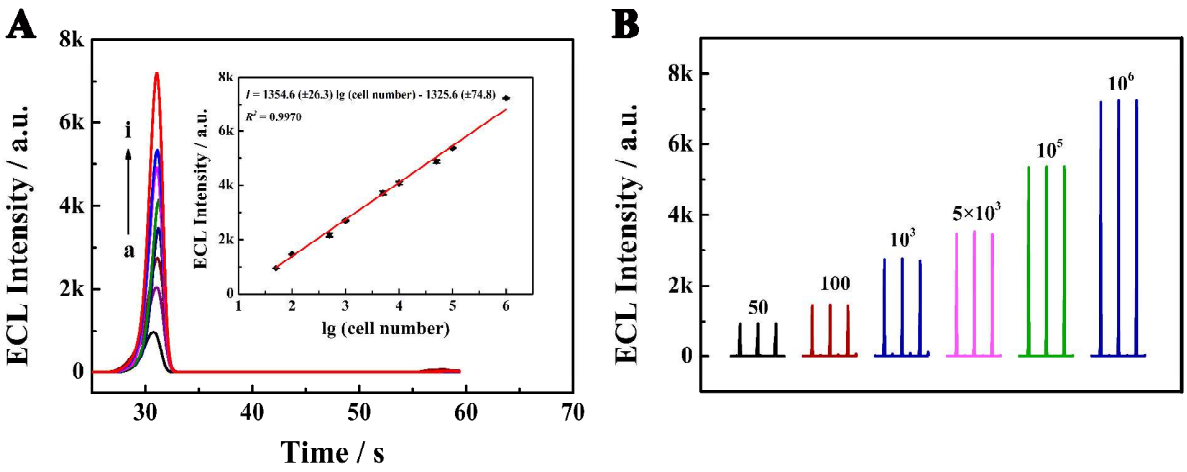

Fig. 4 (A) ECL profiles of the proposed ECL biosensors in different Hela cell numbers: 50, 10^2, 5×10^2, 10^3, 5×10^3, 10^4, 5×10^4, 10^5, 5×10^5, 10^6. The inset shows the logarithmic calibration curve for Hela cell numbers in 0.1 M PBS (pH 7.4). (B) The stability of the proposed ECL biosensor with different Hela cell numbers.

Application of proposed ECL biosensor for Anticancer Drug Screening

For introducing the proposed biosensor to clinical cancer research, the proposed ECL biosensor was applied in the anticancer drug screening. The Hela cells were treated with different concentration of cisplatin for 36 h before detection. Under the effect of cisplatin, the telomerase activity was declined and then the cells were apoptotic. The apoptosis of cisplatin

treated Hela cells were detected by laser confocal microscope that was a standard way to observe the cell state (Fig. S3A, supporting information). The DAPI stained cell nuclear (blue) and annexin V-FITC stained apoptotic cells (green) were observed in the fluorescent images. The fluorescent intensity of DAPI was utilized to represent all the cell in sight. The fluorescent intensity of annexin V-FITC was applied to present the state of apoptotic cells. Besides, these fluorescent images were overlaid as the polychrome images (PCI). It could be clearly seen that the fluorescent intensity of annexin V-FITC increased with the increasing concentration of cisplatin. Here, an apoptotic index was calculated with 11 different images by eq 1, in which the signal degree was the fluorescent intensity of annexin V-FITC with 0−4 levels.[33]

$$\text{Apoptotic index} = \sum \frac{cell\ number_i \times signal\ degree}{total\ cell\ number} \quad (1)$$

The apoptotic index was increased obviously with the increasing of the cisplatin concentration from the Fig. S3B (supporting information), which indicated that the cisplatin has satisficed treatment effect to Hela cells. The regression equation of laser confocal microscope was *Apoptotic index* = 0.00218 $c_{\text{cisplatin}}$ + 0.77542 with a correlation coefficient of 0.9218. Meanwhile, the telomerase activity was decreased with the increasing of the cisplatin concentration, which also indicated that the cisplatin has good treatment effect to Hela cells. The regression equation of proposed method was I = -5.9312 $c_{\text{cisplatin}}$ + 5615.9 with a correlation coefficient of 0.9920, which was higher than that received by laser confocal microscope. These results indicated that the proposed ECL biosensor could become a powerful tool for the cell apoptosis monitoring based anticancer drug screening.

Conclusion

In summary, an ultrasensitive ECL biosensor was fabricated for the determination of telomerase activity by using self-enhanced Ru-PEI complex doped ZIF-8 MOFs as signal indicator. The proposed ECL biosensor performed high sensitivity, stability and board linear range in telomerase activity detection. And the proposed assay provided a novel avenue for raising the utilization ratio of self-enhanced materials, broadened the application of luminescence-functionalized MOFs in analytical chemistry and proposed a feasible way to synthesize luminescence-functionalized MOFs with superior electrochemical stability and excellent ECL property by using luminescent molecules. Moreover, the proposed ECL biosensor presented satisfied applicability for anticancer drug screening, which indicated that the proposed ECL biosensor might be a powerful research tool in analytical chemistry, cancer research and other related fields.

ASSOCIATED CONTENT

Supporting Information.

Experimental details for materials and reagents, apparatus. supplementary figures and tables.

AUTHOR INFORMATION

Corresponding Author

*Email: yuanruo@swu.edu.cn. Tel.: +86-23-68252277. Fax: +86-23-68253172.

yqchai@swu.edu.cn. Tel.: +86-23-68252277. Fax: +86-23-68253172.

Notes

The authors declare no competing financial interest.

ACKNOWLEDGMENT

This work was financially supported by the National Natural Science Foundation (NNSF) of China (51473136, 21575116 and 21675129), and the Fundamental Research Funds for the Central Universities (XDJK2015A002), China

REFERENCES

(1) Nandakumar, J.; Cech, T. R. *Nat. Rev. Mol. Cell Biol.* **2013,** *14,* 69-81.

(2) Nault, J. C.; Mallet, M.; Pilati, C.; Calderaro, J.; Sage, P. B.; Laurent, C.; Laurent, A.; Cherqui, D.; Balabaud, C.; Rossi, J. Z. *Nat. Commun.* DOI: 10.1038/ncomms3218.

(3) Ding, Z. H.; Wu, C. J.; Jaskelioff, M.; Ivanova, E.; Alimova, M. K.; Protopopov, A.; Chu, G. C.; Wang, G. C.; Lu, X.; Larot, E. S.; Hu, J.; Wang, W.; Xiao, Y. H.; Zhang, H. L.; Zhang, J. H.; Zhang, J. F.; Gan, B. Y.; Perry, S. R.; Jiang, S.; Li, L. R.; Horner, J. W.; Wang, Y. A.; Chin, L.; Depinho, R. A. *Cell* **2012,** *148,* 896–907.

(4) Xie, Z. W.; Jay, K. A.; Smith, D. L.; Zhang, Y.; Liu, Z.; Zheng, J. S.; Tian, R. L., Li, H.; Blackburn, E. H. *Cell* **2015,** *160,* 928–939.

(5) Lemieux, B.; Laterreur, N.; Perederina, A.; Noel, J. F.; Dubois, M. L.; Krasilnikov, A. S.; Wellinger, R. J. *Cell* **2016,** *165,* 1171–1181.

(6) Hiyama, E.; Hiyama, K. *Cancer Lett.* **2003,** *194,* 221-223.

(7) Broccoli, D.; Young, J. W.; Lange, T. D.; *Proc. Natl. Acad. Sci.* **1995,** *92,* 9082-9086.

(8) Kim, N. W.; Piatyszek, M. A.; Prowse, K. R.; Harley, C. B.; West, M. D.; Ho, P. L. C.; Coviello, G. M.; Wright, W. E.; Weinrich, S. L.; Shay, J. W. *Science* **1994,** *266,* 2011-2014.

(9) Xu, X. L.; Wei, M.; Liu, Y. J.; Liu, X.; Wei, W.; Zhang, Y. J.; Liu, S. Q. *Biosens. Bioelectron.* **2017,** *87,* 600-606.

(10) Zhang, L.; Zhang, S. J.; Pan, W.; Liang, Q. C.; Song, X. Y. *Biosens. Bioelectron.* **2016,** *77,* 144-148.

(11) Qian, R. C.; Ding, L.; Yan, L. W.; Lin, M. F.; Ju, H. X. *Anal. Chem.* **2014,** *86,* 8642-8648.

(12) Zhuang, Y.; Zhang, M. S.; Chen, B.; Duan, R. X.; Min, X. H.; Zhang, Z. Y.; Zheng, F. X.; Liang, H. G.; Zhao, Z. J.; Lou, X. D.; Xia, F. *Anal. Chem.* **2015,** *87,* 9487-9493.

(13) Qian, R. C.; Ding, L.; Ju, H. X. *J. Am. Chem. Soc.* **2013,** *135,* 13282-13285.

(14) Qian, R. C.; Ding, L.; Yan, L. W.; Lin, M. F.; Ju, H. X. *J. Am. Chem. Soc.* **2014,** *136,* 8205-8208.

(15) Ling, P. H.; Lei, J. P.; Ju, H. X. *Anal. Chem.* **2016,** *88,* 10680-10686.

(16) Ling, P. H.; Lei, J. P.; Jia, L.; Ju, H. X. *Chem. Commun.* **2016,** *52,* 1226-1229.

(17) Eskiocak, U.; Ariksoysal, D. O.; Ozsoz, M.; Oktem, H. A. *Anal. Chem.* **2007,** *79,* 8807-8811.

(18) Wang, W. J.; Li, J. J.; Rui, K.; Gai, P. P.; Zhang, J. R.; Zhu, J. J. *Anal. Chem.* **2015,** *87,* 3019-3026.

(19) Kim, N. W.; Wu, F. *Nucleic Acids Res.* **1997,** *25,* 2595-2597.

(20) Irkham, Watanabe, T., Fiorani, A., Valenti, G., Paolucci, F., Einaga, Y. *J. Am. Chem. Soc.* **2016,** *138,* 15636-15641.

(21) Valenti, G., Rampazzo, E., Bonacchi, S., Petrizza, L.; Marcaccio, M., Montalti, M., Prodi, L., Paolucci, F. *J. Am. Chem. Soc.* **2016,** *138,* 15935-15942.

(22) Kadimisetty, K., Malla, S., Sardesai, N. P., Joshi, A. A., Faria, R. C., Lee, N. H., Rusling, J. F. *Anal. Chem.* **2015,** *87,* 4472-4478.

(23) Wang, L.; Chen, X.; Lu, Y. L.; Liu, C. X.; Yang, W. S. *Carbon* **2015,** *94,* 472-478.

(24) Cayuela, A.; Soriano, M. L.; Carrion, C. C.; Valcarcel, M. *Chem. Commun.* **2016,** *52,* 1311-1326.

(25) Chen, A. Y.; Ma, S. Y.; Zhuo, Y.; Chai, Y. Q.; Yuan, R. *Anal. Chem.* **2016,** *88,* 3203-3210.

(26) Liang, W. B.; Zhuo, Y.; Xiong, C. Y.; Zheng, Y. N.; Chai, Y. Q.; Yuan, R. *Anal. Chem.* **2015,** *87,* 12363-12371.

(27) Wang, H. J.; Yuan Y. L.; Zhuo, Y.; Chai, Y. Q.; Yuan, R. *Anal. Chem.* **2016,** *88,* 2258-2265.

(28) Wang, H. J.; Yuan Y. L.; Zhuo, Y.; Chai, Y. Q.; Yuan, R. *Anal. Chem.* **2016,** *88,* 5797-5803.

(29) Lin, X. M.; Luo, F. Q.; Zheng, L. Y.; Gao, G. M.; Chi, Y. W. *Anal. Chem.* **2015,** *87,* 4864-4870

(30) Lin, X. M.; Gao, G. M.; Zheng, L. Y.; Chi, Y. W.; Chen, G. N. *Anal. Chem.* **2014,** *86,* 1223-1228.

(31) Ma, H. M., Li, X. J., Yan, T., Li, Y., Zhang, Y., Wu, D., Wei, Q., Du, B. *Biosens. Bioelectron.* **2016,** *79*, 379-385.

(32) Xu, Y., Yin, X. B., He, X. W., Zhang, Y. K. *Biosens. Bioelectron.* **2015,** *68*, 197-203.

(33) Huang, X., Huang, X. P., Zhang, A., Zhuo, B. R., Lu, F. S., Chen, Y. W., Gao, W. H. *Biosens. Bioelectron.* **2015,** *70*, 441-446.

(34) Zhang, Z. J.; Wang, Q. L.; Li, P.; Zhou, Y.; Li, S. H.; Yi, W. J.; Chen, A.; Kong, P. Y.; Hu, C. M. *Cancer Epidemiol.* **2009,** *33,* 130−136.

Table of Contents